

Traversable wormholes from massless conformally coupled scalar fields

Carlos Barceló and Matt Visser

Physics Department, Washington University, St. Louis, Missouri 63130-4899, USA.

9 August 1999; L^AT_EX-ed October 29, 2013

Abstract

The massless conformally coupled scalar field is characterized by the so-called “new improved stress-energy tensor”, which is capable of classically violating the null energy condition. When coupled to Einstein gravity we find a three-parameter class of exact solutions. These exact solutions include the Schwarzschild geometry, assorted naked singularities, and a large class of traversable wormholes.

Keywords: Traversable wormholes, energy conditions, classical solutions.

1 Introduction

The equations of general relativity relate the geometry of a spacetime manifold to its matter content. Given a geometry one can find the distribution of mass-energy and momenta that support it. Unless there are restrictions on the features that the matter content can possess, general relativity allows the existence of spacetime geometries in which apparently distant regions of space are close to each other through wormhole connections. The existence or not of traversable wormhole geometries has many implications that could change our way of looking at the structure of spacetime (see [1] for a survey and bibliography on the subject).

The analysis of M. Morris and K. Thorne [2] regarding traversable wormhole geometries showed that, in order for the flaring out of geodesics characteristic of a Lorentzian wormhole throat to happen, it is necessary that the matter that supports the wormhole throat be peculiar: it has to violate the Null Energy Condition (NEC) [3]. That is to say, even a null geodesic observer would see negative energy densities on passing the throat. This analysis was originally done with static spherically symmetric configurations, but the NEC violation is a generic property of an arbitrary wormhole throat [4].

It is often (mistakenly) thought that classical matter always satisfies NEC. By contrast, in the quantum regime there are well-known situations in which NEC violations can easily be obtained [1]. For this reason, most investigations regarding wormhole physics are developed within the realm of semiclassical gravity, where the expectation value of the quantum energy-momentum tensor is used as the source for the gravitational field [5].

However, one can easily see that the energy-momentum tensor of a scalar field conformally coupled to gravity can violate NEC even at the classical level [6]. We would like to highlight that this energy-momentum tensor is the most natural one for a scalar field at low energies (energies well below the Planck scale, or any other scale below which a scalar field theory might become non-renormalizable), because its matrix elements are finite in every order of renormalized perturbation theory [7]. In flat spacetime, this energy-momentum tensor defines the same four-momentum and Lorentz generators as that associated with a minimally coupled scalar field and, in fact, it was first constructed as an improvement of the latter [7]. Thus, we wish to focus attention on the so-called “new improved energy-momentum tensor” of particle physics. At higher energies, still well below the Planck scale, there may also be other forms of classical violations of the NEC, such as higher derivative theories [8, 9], Brans–Dicke theory [10, 11], or even more exotic possibilities.¹

In this paper, we will concentrate on the massless conformally coupled scalar field. We will explicitly show that it can provide us with the flaring out condition characteristic of traversable wormholes. We have analytically solved the Einstein equations for static and spherically symmetric geometries. We find a three-parameter class of exact solutions. These solutions include the Schwarzschild geometry, certain naked singularities, and a collection of traversable wormholes. However, in all these wormhole geometries the effective Newton’s constant has a different sign in the two asymptotic regions. At the end of the paper we will briefly discuss some ways of escaping from this somewhat disconcerting conclusion.

2 Einstein conformal scalar field solutions

In this section, we will describe the exact solutions to the combined system of equations for Einstein gravity and a massless conformally coupled scalar field, in the simple case of static and spherically symmetric configurations.

The Einstein equations can be written as $\kappa G_{\mu\nu} = T_{\mu\nu}$, where $G_{\mu\nu} = R_{\mu\nu} - \frac{1}{2}g_{\mu\nu}R$ is the Einstein tensor, with $R_{\mu\nu}$ the Ricci tensor and R the scalar curvature. $T_{\mu\nu}$ is the energy-momentum tensor of the matter field, and $\kappa = (8\pi G_N)^{-1}$, with G_N denoting Newton’s constant. For a massless conformal scalar field ϕ_c , the energy-momentum tensor acquires the form [6]

$$T_{\mu\nu} = \nabla_\mu \phi_c \nabla_\nu \phi_c - \frac{1}{2}g_{\mu\nu}(\nabla\phi_c)^2 + \frac{1}{6} \left[G_{\mu\nu} \phi_c^2 - 2 \nabla_\mu(\phi_c \nabla_\nu \phi_c) + 2 g_{\mu\nu} \nabla^\lambda(\phi_c \nabla_\lambda \phi_c) \right], \quad (2.1)$$

with the field satisfying the equation $(\nabla^2 - \frac{1}{6}R)\phi_c = 0$. This is the generalization to curved spacetime of the “new improved energy-momentum tensor” more usually invoked in a particle physics context [7].

The key feature of the energy-momentum tensor for a conformal field is that it is traceless, $T_{\mu\nu} g^{\mu\nu} = 0$, and therefore $R = 0$. For this reason, we can write the coupled

¹ For instance, we mention the work by H. Ellis [12] in which he considered changing the sign in front of the energy-momentum tensor for a minimally coupled scalar field. Reversing this sign from the usual one, he found classical wormhole solutions, which with hindsight is not surprising since reversing the energy-momentum tensor explicitly violates the energy conditions. This paper is of particular interest since it pre-dates the Morris–Thorne analysis by 15 years.

Einstein plus *conformal* scalar field equations as

$$R_{\mu\nu} = \left(\kappa - \frac{1}{6} \phi_c^2 \right)^{-1} \left(\frac{2}{3} \nabla_\mu \phi_c \nabla_\nu \phi_c - \frac{1}{6} g_{\mu\nu} (\nabla \phi_c)^2 - \frac{1}{3} \phi_c \nabla_\mu \nabla_\nu \phi_c \right), \quad (2.2)$$

$$\nabla^2 \phi_c = 0. \quad (2.3)$$

We are interested in static and spherically symmetric solutions of these equations. In order to find these solutions, we will start by looking for metrics conformally related to the Janis–Newman–Winicour–Wyman (JNWW) [13, 14, 15] static spherically symmetric solutions of the Einstein *minimally coupled* massless scalar field equations:

$$R_{\mu\nu} = \kappa^{-1} (\nabla_\mu \phi_m \nabla_\nu \phi_m), \quad (2.4)$$

$$\nabla^2 \phi_m = 0. \quad (2.5)$$

The JNWW solutions can be expressed [17] as

$$ds_m^2 = - \left(1 - \frac{2\eta}{r} \right)^{\cos \chi} dt^2 + \left(1 - \frac{2\eta}{r} \right)^{-\cos \chi} dr^2 + \left(1 - \frac{2\eta}{r} \right)^{1-\cos \chi} r^2 (d\theta^2 + \sin^2 \theta d\Phi^2), \quad (2.6)$$

$$\phi_m = \sqrt{\frac{\kappa}{2}} \sin \chi \ln \left(1 - \frac{2\eta}{r} \right). \quad (2.7)$$

The JNWW solutions possess obvious symmetries under $\chi \rightarrow -\chi$, (with $\phi_m \rightarrow -\phi_m$). Less obvious is that by making a coordinate transformation $r \rightarrow \tilde{r} = r - 2\eta$, one uncovers an additional symmetry under $\{\eta, \chi\} \rightarrow \{-\eta, \chi + \pi\}$, (with $\phi_m \rightarrow +\phi_m$). In view of these symmetries one can without loss of generality take $\eta \geq 0$ and $\chi \in [0, \pi]$. Similar symmetries will be encountered for conformally coupled scalars.²

The requirement that a metric conformal to the JNWW metric, $ds = \Omega(r) ds_m$ with $\Omega(r)$ the conformal factor, have a zero scalar curvature [necessary if it has to be solution of the system of equations (2.2)], easily provides a second-order differential equation for the conformal factor as a function of ϕ_m :

$$\frac{d^2 \Omega(\phi_m)}{d\phi_m^2} = \frac{1}{6\kappa} \phi_m. \quad (2.8)$$

Its solutions can be parametrized in the form

$$\Omega = \alpha_+ \exp \left(+\phi_m / \sqrt{6\kappa} \right) + \alpha_- \exp \left(-\phi_m / \sqrt{6\kappa} \right), \quad (2.9)$$

with α_+ and α_- two real constants. The equation $\nabla^2 \phi_c = 0$ can now be integrated yielding

$$\phi_c = A \frac{\sqrt{6\kappa}}{4\alpha_+ \alpha_-} \left[\frac{\alpha_+ \exp \left(+\phi_m / \sqrt{6\kappa} \right) - \alpha_- \exp \left(-\phi_m / \sqrt{6\kappa} \right)}{\alpha_+ \exp \left(+\phi_m / \sqrt{6\kappa} \right) + \alpha_- \exp \left(-\phi_m / \sqrt{6\kappa} \right)} \right] + B, \quad (2.10)$$

² The key to this symmetry is to realise that

$$\left(1 - \frac{2\eta}{r} \right) = \left(1 + \frac{2\eta}{\tilde{r}} \right)^{-1}.$$

where A and B are two additional integration constants.

In order that the metric and conformal scalar field just found be solutions of the whole set of equations (2.2), the four integration constants, α_+ , α_- , A , and B , must be inter-related in a specific way. After a little algebra the equation for the tt component in (2.2) implies the following relations³

$$A B \alpha_+ \alpha_- = 0, \quad (2.11)$$

$$\alpha_+^2 \alpha_-^2 \left(1 - \frac{B^2}{6\kappa} \right) + \frac{A^2}{16} = 0. \quad (2.12)$$

Therefore, we have two options:

Case i) $B = 0$, $A = \pm 4 \alpha_+ \alpha_-$;

$$\Omega = \alpha_+ \exp\left(+\phi_m/\sqrt{6\kappa}\right) + \alpha_- \exp\left(-\phi_m/\sqrt{6\kappa}\right), \quad (2.13)$$

$$\phi_c = \pm\sqrt{6\kappa} \left[\frac{\alpha_+ \exp\left(+\phi_m/\sqrt{6\kappa}\right) - \alpha_- \exp\left(-\phi_m/\sqrt{6\kappa}\right)}{\alpha_+ \exp\left(+\phi_m/\sqrt{6\kappa}\right) + \alpha_- \exp\left(-\phi_m/\sqrt{6\kappa}\right)} \right]. \quad (2.14)$$

Case ii) $A = 0$, $B = \pm\sqrt{6\kappa}$;

$$\Omega = \alpha_+ \exp\left(+\phi_m/\sqrt{6\kappa}\right) + \alpha_- \exp\left(-\phi_m/\sqrt{6\kappa}\right), \quad (2.15)$$

$$\phi_c = \pm\sqrt{6\kappa}. \quad (2.16)$$

Notice that these two branches of solutions intersect when either α_+ or α_- are equal to zero.

The set of solutions we have found is a generalization of the solutions found by Froyland [16], and some time later by Agnese and La Camera [17]. Indeed, in the case $\alpha_+ = \alpha_-$ the conformal factor becomes $\Omega = \cosh(\phi_m/\sqrt{6\kappa})$, (we drop a unimportant constant factor), and the field $\phi_c = \pm\sqrt{6\kappa} \tanh(\phi_m/\sqrt{6\kappa})$, in agreement with the expression given by Agnese and La Camera. The Froyland solution is in fact identical to that of Agnese–La Camera though this is not obvious because Froyland chose to work in Schwarzschild coordinates. Because of this, Froyland could only provide an implicit (rather than explicit) solution.⁴

Let us now analyze the different behaviours of these solutions. For this task, it is convenient to look at the conformal factor as a function of r ,

$$\Omega(r) = \alpha_+ \left(1 - \frac{2\eta}{r} \right)^{\frac{\sin \chi}{2\sqrt{3}}} + \alpha_- \left(1 - \frac{2\eta}{r} \right)^{-\frac{\sin \chi}{2\sqrt{3}}}. \quad (2.17)$$

³ In view of the assumed static and spherical symmetries, the Einstein equations provide only three constraints, and by the contracted Bianchi identities only two of these are independent. Thus it is only necessary to consider the trace R and the tt component $R_{\hat{t}\hat{t}}$ to guarantee a solution of the entire tensor equation.

⁴ That is, Froyland calculated $\mathcal{R}(\phi_c)$, which in Schwarzschild coordinates is not analytically invertible to provide $\phi_c(\mathcal{R})$. The coordinate system chosen by Agnese and La Camera is much better behaved in this regard and $\phi_c(r)$ can be explicitly calculated as we have seen above. The trade-off is that whereas $\mathcal{R}(r)$ can be written down explicitly, there is no way of analytically inverting this function to get $r(\mathcal{R})$.

In the same way, as a function of r , the Schwarzschild radial coordinate \mathcal{R} has the form

$$\mathcal{R}(r) = r \left(1 - \frac{2\eta}{r}\right)^{\frac{1-\cos\chi}{2}} \Omega(r). \quad (2.18)$$

If we define an angle Δ by $\tan(\Delta/2) = (\alpha_+ - \alpha_-)/(\alpha_+ + \alpha_-)$, then the domain $\Delta \in (-\pi, \pi]$ exhausts all possible metric configurations, as a constant overall factor in the metric can be absorbed in the definition of coordinates. We have a three-parameter family of solutions depending on η , the angle Δ , and the angle $\chi \in (-\pi, \pi]$. In fig. 1 we have drawn the parameter space as a square. Indeed, parallel edges are identified, so the parameter space is an orbifold (a two-torus subjected to symmetry identifications). In fact, the solution space is invariant if we change $\{\eta, \chi, \Delta\}$ to $\{\eta, -\chi, -\Delta\}$. Furthermore, the coordinate transformation $r \rightarrow \tilde{r} = r - 2\eta$ can now be used to deduce an invariance under $\{\eta, \chi, \Delta\} \rightarrow \{-\eta, \chi + \pi, \Delta\}$. Combining the two symmetries, we deduce an invariance under $\{\eta, \chi, \Delta\} \rightarrow \{-\eta, \pi - \chi, -\Delta\}$. Thus without loss of generality we only have to deal with the region $\eta \geq 0$ with $\chi \in [0, \pi]$. Also, we need only consider the geometries in which $\Delta \neq \pi$ because, for that value, the geometries do not have an asymptotic flat region when r approaches infinity.⁵

For the rest of parameter space, an analysis when r approaches 2η of the behaviour of the tt component of the Ricci tensor ($R_{\hat{t}\hat{t}}$ in an orthonormal coordinate basis) shows that it diverges for every point in parameter space except when $\chi = 0$, $\{\chi = \frac{\pi}{3}, \Delta \neq \frac{\pi}{2}\}$, $\{\chi = \frac{2\pi}{3}, \Delta = \frac{\pi}{2}\}$, or $\chi = \pi$. Thus, except for these parameter values, we have geometries with a naked curvature singularity at $r = 2\eta$.

Among these singular geometries, those with $0 < \chi < \frac{\pi}{3}$ and $\Delta \neq \frac{\pi}{2}$ deserve additional attention. For them, the Schwarzschild radial coordinate blows up when approaching $r = 2\eta$. They are geometries with wormhole shape, but with something “strange” in the other “asymptotic” region. We can easily check that the proper radial distance between every point $r > 2\eta$ and $r = 2\eta$ is finite. Also the proper volume beyond every sphere at finite $r > 2\eta$ is itself finite, even though the proper area of the spherical sections diverges as one approaches $r = 2\eta$. Therefore, although one certainly encounters a flare-out (a wormhole throat) before reaching $r = 2\eta$, we cannot speak properly of another asymptotic region.⁶

⁵ We mention in particular that the physical scale length, effective Newton constant, and physical mass of the spacetime can be isolated from a weak-field expansion near spatial infinity. We find

$$G_{\text{eff}} M = \eta \left(\cos\chi + \tan\left[\frac{\Delta}{2}\right] \frac{\sin\chi}{\sqrt{3}} \right).$$

We note that this scale length is invariant under all the symmetries mentioned above (as it must be). The effective Newton constant is

$$G_{\text{eff}} = \frac{1}{8\pi(\kappa - \frac{1}{6}\phi_\infty^2)} = \frac{1}{8\pi\kappa} \left(1 - \tan^2\frac{\Delta}{2}\right)^{-1}.$$

Thus G_{eff} , M , and $G_{\text{eff}} M$ are separately invariants of the symmetries discussed above. For the objectional value $\Delta = \pi$, the lack of an asymptotically flat region is reflected in an infinite physical mass.

⁶ Thus these geometries are certainly Lorentzian wormholes, and could even be called “traversable in principle”, but because of the nasty behaviour on the other side of the wormhole throat, they do not deserve to be called “traversable in practice”.

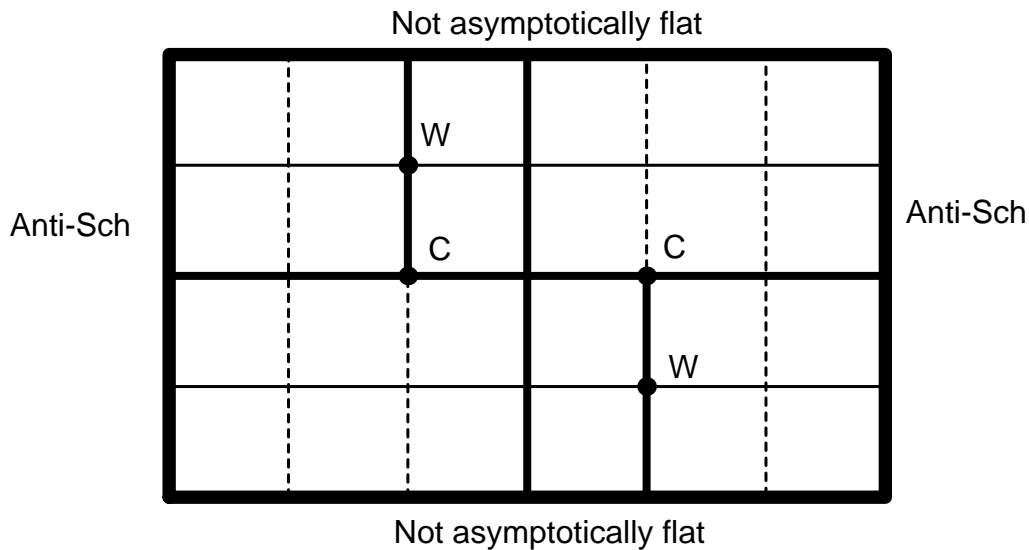


Figure 1: Sketch of the parameter space of our class of solutions to Einstein gravity coupled to the “new improved stress-energy tensor”. Using the symmetries discussed in the text we have taken $\eta \geq 0$. We sketch the range $\chi \in [-\pi, +\pi]$ and $\Delta \in [-\pi, +\pi]$. Parameter space is an orbifold because of the remaining symmetry under $\{\eta, \chi, \Delta\}$ to $\{\eta, -\chi, -\Delta\}$. The left and right borders of the figure correspond to anti-Schwarzschild space (the negative mass Schwarzschild geometry), while the top and bottom borders correspond to spacetimes that are not asymptotically flat. The central vertical line corresponds to the Schwarzschild black hole, while the central horizontal line represents the Froyland–Agnese–La Camera branch of solutions. The two offset vertical branches are the special class of traversable wormholes with two asymptotically flat regions that are the main focus of this paper. These branches terminate in “cornucopia” labelled C , and contain the special symmetric traversable wormholes labelled W .

The first non singular case is $\chi = 0$. In this case we recover the Schwarzschild black hole geometry. This geometry, of course, does not have a curvature singularity at $r = 2\eta$, just a coordinate singularity. It is instead singular at $r = 0$.

For the special cases $\{\chi = \frac{\pi}{3}, \Delta \neq \frac{\pi}{2}\}$ there exist situations in which the Schwarzschild radial coordinate \mathcal{R} and the gravitational potential g_{tt} go to non-zero constants when approaching $r = 2\eta$. This suggests that we might be able to extend the geometry beyond $r = 2\eta$. We leave for the next section the analysis of how this extension can be done, showing that there exist genuine wormhole solutions.

In the case $\{\chi = \frac{2\pi}{3}, \Delta = \frac{\pi}{2}\}$ we can write the metric as

$$ds^2 = -dt^2 + \left(1 - \frac{2\eta}{r}\right) dr^2 + (r - 2\eta)^2(d\theta^2 + \sin^2\theta d\Phi^2). \quad (2.19)$$

Writing $\tilde{r} = r - 2\eta$, so that

$$ds^2 = -dt^2 + \frac{d\tilde{r}^2}{\left(1 + \frac{2\eta}{\tilde{r}}\right)} + \tilde{r}^2(d\theta^2 + \sin^2\theta d\Phi^2), \quad (2.20)$$

a brief calculation shows that this geometry is also singular at $\tilde{r} = 0$, $r = 2\eta$, even though $R_{\tilde{t}\tilde{t}}$ remains finite there. (The other Ricci components, $R_{\tilde{r}\tilde{r}}$ and $R_{\tilde{\theta}\tilde{\theta}}$, diverge as $\tilde{r} \rightarrow 0$.)

Finally, the case $\chi = \pi$ corresponds to a negative mass Schwarzschild geometry. It has a naked curvature singularity at $r = 2\eta$, but after the coordinate change $r \rightarrow \tilde{r} = r - 2\eta$, the naked curvature singularity moves to $\tilde{r} = 0$, and the character of the geometry becomes obvious.

3 Traversable wormhole solutions

This section is devoted to the analysis of the case $\{\chi = \frac{\pi}{3}, \Delta \neq \frac{\pi}{2}\}$. For this task, it is convenient to change to isotropic coordinates

$$r = \bar{r} \left(1 + \frac{\eta}{2\bar{r}}\right)^2. \quad (3.21)$$

With the new radial coordinate running from $\bar{r} = \eta/2$ to ∞ we cover the same portion of the metric manifold that $r \in [\eta, \infty)$ did before. However, can the manifold be analytically extended beyond $\bar{r} = \eta/2$? The answer is yes. We can write the metric in isotropic coordinates as

$$ds^2 = \left[\alpha_+ \frac{\left(1 - \frac{\eta}{2\bar{r}}\right)}{\left(1 + \frac{\eta}{2\bar{r}}\right)} + \alpha_- \right]^2 \left[-dt^2 + \left(1 + \frac{\eta}{2\bar{r}}\right)^4 [d\bar{r}^2 + \bar{r}^2(d\theta^2 + \sin^2 \theta d\Phi^2)] \right], \quad (3.22)$$

noticing that it is perfectly well behaved at $\bar{r} = \eta/2$. We want to point out that for $0 < \bar{r} < \eta/2$ the conformal factor Ω^2 is real and negative, while the JNWW solution is ill-behaved in the sense that the metric ds_m^2 has opposite signature to the usual. Nevertheless, the metric ds^2 is perfectly well behaved. Thus, strictly speaking, only the region $\bar{r} > \eta/2$ is conformally related with its corresponding JNWW solution.

Among these solutions, in those with $\Delta \in (-\pi, 0)$ the Schwarzschild radial coordinate $\mathcal{R}(\bar{r})$ reaches a minimum value at $\bar{r} = (\eta/2) |\tan(\Delta/2)|^{1/2}$, and comes back to infinity at $\bar{r} = 0$, showing up as another asymptotically flat region. As well as this, the tt component of the metric is everywhere non-zero. Therefore, the region in parameter space $\{\chi = \frac{\pi}{3}, \Delta \in (-\pi, 0)\}$ represents genuine traversable wormhole solutions, with the throat of the wormhole being located at $\bar{r} = (\eta/2) |\tan(\Delta/2)|^{1/2}$. For completeness, in the solution with $\Delta = 0$, $\mathcal{R}(\bar{r})$ reaches a minimum at $\bar{r} = 0$, but this sphere is at a infinite proper distance from every other \bar{r} so we can conclude that this geometry is a ‘‘cornucopia’’ (tube without end). ($\Delta = -\pi$ represents the reversed cornucopia with no asymptotic region at $\bar{r} = \infty$). For the remaining values of $\Delta \in (0, \pi)$ the geometry pinches off (the conformal prefactor in equation (3.22) goes to zero) at finite positive radius $\bar{r} = (\eta/2) \tan(\Delta/2)$.

We have seen that a scalar field coupled conformally to gravity can support wormhole geometries. On these wormhole configurations the conformal scalar field takes the following form

$$\phi_c = \pm \sqrt{6\kappa} \frac{\alpha_+ \left(1 - \frac{\eta}{2\bar{r}}\right) - \alpha_- \left(1 + \frac{\eta}{2\bar{r}}\right)}{\alpha_+ \left(1 - \frac{\eta}{2\bar{r}}\right) + \alpha_- \left(1 + \frac{\eta}{2\bar{r}}\right)}. \quad (3.23)$$

It is a monotonically increasing or decreasing function (depending on the overall sign) between one asymptotic region and the other, taking the values

$$\phi_c|_{\text{asym}_1} = \pm\sqrt{6\kappa} \tan \frac{\Delta}{2}, \quad \text{and} \quad \phi_c|_{\text{asym}_2} = \pm \frac{\sqrt{6\kappa}}{\tan \frac{\Delta}{2}}. \quad (3.24)$$

This monotonic behaviour for the scalar field causes an asymmetry between the asymptotic regions. In fact, we can realize of the real importance of this asymmetry by looking at the effective Newton's constant, $G_{\text{eff}} = 8\pi(\kappa - \frac{1}{6}\phi_c^2)^{-1}$, that can be defined on these systems. It not only reaches a different value on each asymptotic region,

$$G_{\text{eff}}|_{\text{asym}_1} = \frac{1}{8\pi\kappa} \frac{1}{(1 - \tan^2 \frac{\Delta}{2})}, \quad G_{\text{eff}}|_{\text{asym}_2} = -\frac{1}{8\pi\kappa} \frac{\tan^2 \frac{\Delta}{2}}{(1 - \tan^2 \frac{\Delta}{2})}, \quad (3.25)$$

it also reaches a different *sign*. From the point of view of the asymptotic region with a positive effective Newton's constant, the wormhole throat is located in the region in which G_{eff} has already changed its sign. This asymmetry is reflected also in the values of the asymptotic masses measured on the two sides of the wormhole throat. The scale lengths are

$$(G_{\text{eff}}M)|_{\text{asym}_1} = \frac{\eta}{2} \left(1 + \tan \frac{\Delta}{2}\right), \quad (G_{\text{eff}}M)|_{\text{asym}_2} = \frac{\eta}{2} \left(1 + \frac{1}{\tan \frac{\Delta}{2}}\right). \quad (3.26)$$

The observers in the asymptotic region with a positive G_{eff} see a positive asymptotic mass, while those in the other asymptotic region see a negative G_{eff} and a positive asymptotic mass. The case $\Delta = -\frac{\pi}{2}$ corresponds to $\alpha_+ = 0$, so

$$ds^2 = -dt^2 + \left(1 + \frac{\eta}{2\bar{r}}\right)^4 [d\bar{r}^2 + \bar{r}^2(d\theta^2 + \sin^2\theta d\Phi^2)], \quad (3.27)$$

$$\phi_c = \pm\sqrt{6\kappa}. \quad (3.28)$$

This describes a limiting symmetric wormhole with an everywhere zero effective Newton's constant and both asymptotic masses equal to zero.

These asymmetric features are disappointing because we would like to have wormholes connecting equivalent regions of space. At this point we have to say that while a conformal scalar field can provide us with the “flaring out” condition for geodesics, it has the drawback of reversing the sign of the effective Newton's constant in the other asymptotic region.

4 Discussion

We have found that, among the classical solutions of general relativity coupled to a massless conformal scalar field there exist genuine Lorentzian traversable wormhole geometries. Although perfectly well behaved from a geometrical point of view, they are asymmetric in the sense that the effective Newton's constant has a different sign in each asymptotic region.

Inspecting the expression for the Laplacian of a scalar field in a static and spherically symmetric geometry

$$\nabla^2 \phi_c = \frac{1}{\sqrt{-g}} \partial_r \left[\sqrt{-g} g^{rr} \partial_r \phi_c \right], \quad (4.29)$$

we see that in order for the scalar field to be able to change its monotonic behaviour in a non-singular geometry, there must be some points at which $\nabla^2 \phi_c \neq 0$. This suggests that in more general situations than those analyzed in this paper we could find traversable wormhole solutions with no asymmetry between the asymptotic regions. For example, if we add to our system a quantity of normal matter with a positive trace for the energy-momentum tensor ($T > 0$), and we place this normal matter in two thin spherical shells (see fig. 2), we can join smoothly an inner region with the geometry of the symmetric wormhole solution (3.27) to two outer asymptotic geometries, both with positive effective Newton's constants.⁷ The requirement that $T > 0$ in the shells translates into a localized negative scalar curvature, $R < 0$, necessary for bringing down the value of the scalar field from that in the inner region.

Finally, we conclude by emphasising that it is not so much the occurrence of classical wormholes in and of themselves that is the main surprise of this paper. Rather, what is truly surprising here is that such an inoffensive and physically well-motivated classical source, the “new improved stress-energy tensor”, leads to classical traversable wormholes.

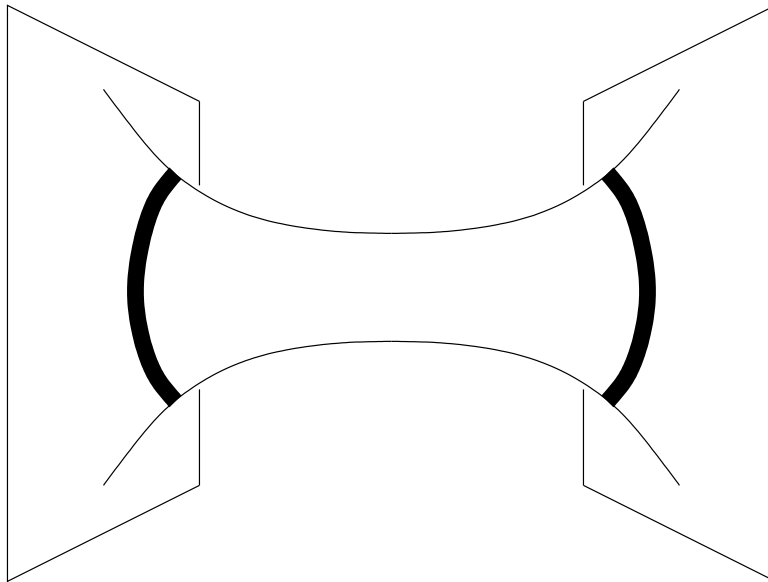


Figure 2: Schematic depiction of how two thin shells of ordinary matter could be combined with the flare out effect coming from the “new improved stress-energy tensor” to build a traversable wormhole that has nice asymptotic properties on both sides of the wormhole throat. The geometry is piecewise a solution of the field equations discussed in this paper, with a thin shell of normal stress-energy being used to start the scalar field moving downwards from $\phi_c = \sqrt{6\kappa}$.

⁷ Thus we are considering geometries that are built piecewise out of segments of the solutions considered in this paper, with junction conditions applied at the thin shells.

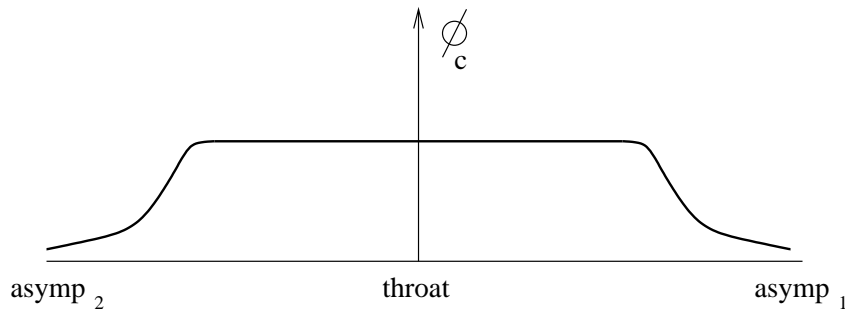


Figure 3: Schematic depiction of the scalar field ϕ_c as a function of position as one traverses the throat of this “cut and paste” wormhole.

Acknowledgments

The research of CB was supported by the Spanish Ministry of Education and Culture (MEC). MV was supported by the US Department of Energy.

References

- [1] M. Visser, *Lorentzian wormholes: from Einstein to Hawking*, (American Institute of Physics, Woodbury, 1995).
- [2] M.S. Morris and K.S. Thorne, *Am. J. Phys.* **56** (1988) 395.
- [3] S.W. Hawking and G.F.R. Ellis, *The large scale structure of space-time*, (Cambridge University Press, England, 1973).
- [4] D. Hochberg and M. Visser, *Phys. Rev. Lett.* **81** (1998) 746.
- [5] D. Hochberg, A. Popov, S.V. Sushkov, *Phys. Rev. Lett.* **78** (1997) 2050.
- [6] E.E. Flanagan and R.M. Wald, *Phys. Rev.* **D54** (1996) 6233.
- [7] C.G. Callan, S. Coleman, and R. Jackiw, *Ann. Phys.* **59** (1970) 42.
- [8] D. Hochberg, *Phys. Lett.* **B251** (1990) 349.
- [9] K. Ghoroku and T. Soma, *Phys. Rev.* **D46** (1992) 1507.
- [10] A. Agnese and M. La Camera, *Phys. Rev.* **D51** (1995) 2011.
- [11] L.A. Anchordoqui, M.L. Trobo, H. Vucetich, and F. Zyserman, *Gravitational memory of natural wormholes*, gr-qc/9906119, and references therein.
- [12] H.G. Ellis, *J. Math. Phys.* **14** (1973) 104.
- [13] A. I. Janis, E. T. Newman, and J. Winicour, *Phys. Rev. Lett.* **20** (1968) 878.
- [14] M. Wyman, *Phys. Rev.* **D24** (1981) 839.

- [15] K. S. Virbhadra, *Int. J. Mod. Phys. A* **12** (1997) 4831.
- [16] J. Froyland, *Phys. Rev.* **D25** (1982) 1470.
- [17] A. Agnese and M. La Camera, *Phys. Rev.* **D31** (1985) 1280.